Oxygen sensing and transport properties of nanofibers of silica, bismuth doped silica and bismuth silicate prepared via electrospinning

CrossMark

Matloob Hussain [1], Syeda Sitwat Batool [1], Z. Imran, Mushtaq Ahmad, Kamran Rasool, M.A. Rafiq *, M.M. Hasan

Micro and Nano Devices Group, Department of Metallurgy and Materials Engineering, Pakistan Institute of Engineering and Applied Sciences, PO Nilore, Islamabad 45650, Pakistan

ARTICLE INFO

ABSTRACT

Electrical measurements as a diagnostic tool for gas sensing application were investigated of the SiO_2 nanofibers, bismuth doped SiO_2 nanofibers and bismuth silicate ($Bi_4(SiO_4)_3$) nanofibers, which were synthesized by electrospinning. The gas sensing devices were fabricated using thermally evaporated Ni–Cr metals on the glass substrate and then nanofibers were deposited between the contact electrodes. The performance of the sensors was evaluated by recording DC and AC measurements in an oxygen (O_2) rich environment. The morphology and structural characterization of nanofibers were characterized by scanning electron microscopy (SEM) and X-ray diffraction (XRD). $Bi_4(SiO_4)_3$ nanofibers exhibited excellent oxygen sensing properties at all temperatures (25–127 °C). The rapid response time (∼49 s) and recovery time (∼9 s) with high linearity indicated that $Bi_4(SiO_4)_3$ nanofibers could be a good candidate for developing practical oxygen gas sensors.

© 2013 Elsevier B.V. All rights reserved.

1. Introduction

To resolve environmental and health issues, significant efforts in the field of research have been initiated. For many years, the interest has been focused on detection and minimization of oxygen emissions from various industrial sources [1–5]. Oxygen sensors have played an important role in food processing plants, biomedicine applications, control of chemical processes and pollution control through automobile engine management [5]. It is observed that the efficiency of an automobile engine is increased with theoretical air–fuel ratio (A/F ≈ 14.7) and the emission of harmful gases such as CO, NO_x and hydrocarbons are also reduced. Therefore, oxygen sensors are developed to control the A/F ratio in order to minimize the gas emissions and to improve the engine efficiency [6]. So, the need for simple, low cost, stable and highly sensitive oxygen sensors has been increased. In the last few years [7] transition metal doped nanomaterial with wide band gap are being extensively used for sensing applications due to their change in electrical properties upon exposure to the gas. Moreover, the quasi-one dimensional materials offer high surface to volume ratio with no grain boundary which is advantageous for high sensitivity and stability of devices, respectively [8].

Silica (SiO_2), a kind of insulator with porous nature has a fast oxygen response time and recovery time. But due to its poor linearity with high impedance values, SiO_2 does not gain much attention in gas sensing industries. It is observed that doping of transition metal in the sensing material could improve the overall sensing response [7]. Herein resistive type oxygen sensors are developed using SiO_2 nanofibers, Bismuth doped SiO_2 nanofibers $Bi_4(SiO_4)_3$ nanofibers. SiO_2 is thermally and chemically stable material, which exhibits insulating properties and widely used as insulation material in the semiconductor industry, but here with the bismuth (Bi) doping it behaves like n-type semiconductor material. The oxygen sensing is measured by varying the oxygen flow rates in the testing chamber. The working of the sensor is characterized by gas response, the response and recovery time and temperature dependent gas response.

2. Experimental

2.1. Sample preparation

Our group [9–12] has done much work on synthesis of ceramic nanofibers using electrospinning. We have reported the synthesis of TiO_2, SiO_2 and $CdTiO_3$ nanofibers. Herein

* Corresponding author. Tel.: +92 51 2207381; fax: +92 51 2208070.
E-mail addresses: zahid.imran733@yahoo.com (Z. Imran), aftab@cantab.net (M.A. Rafiq).
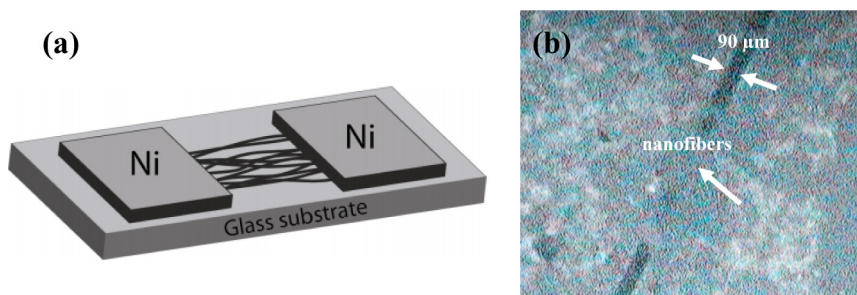[1] These two authors contributed equally.

Fig. 1. (a) Schematic diagram of gas sensing device and (b) optical image of gas sensing device.

nanofibers used for gas sensing has been synthesized by the same route. Polyvinylpyrrolidone (PVP, Mw = 1,300,000), tetraethoxysilane (TEOS) >98%, ethanol (C_2H_5OH > 98%) and acetic acid (CH_3COOH > 98%) were used as starting materials. 13% PVP/ethanol and 13% TEOS/acetic acid solutions were prepared for the synthesis of SiO_2 nanofibers. Bismuth acetate was used for synthesis of xBi–$(1 − x)SiO_2$ nanofibers with $x = 0.01$ and $Bi_4(SiO_4)_3$ nanofibers. A certain amount of bismuth acetate ($Bi(C_2H_3O_2)_3$) was dissolved in 1 ml of N,N-dimethylformamide (DMF) in a capped beaker, then required amount of acetic acid and tetraethoxysilane (TEOS) were added into the mixture (molar ratio of Bi:Si was 0.01:0.99 and 0.5:0.5). The mixture was stirred for 30 min, after that13% polyvinylpyrrolidone (PVP)/ethanol (PVP, Mw ∼ 1,300,000) was slowly added. After being stirred for 90 min, the solution was loaded in a syringe. High voltage (10 kV) was applied to tip of the needle and collector plate [13]. As spun PVP/SiO_2 and Bi doped PVP/SiO_2 nanofibers were collected on an aluminium foil placed on a collector plate. The as collected nanofibers were left in the air for 24 h for hydrolysis of TEOS and annealed at 600 °C for 6 h in the air. The sensing materials were characterized using scanning electron microscopy, energy dispersive spectroscopy (EDX) and X-ray diffraction (XRD).

2.2. Device fabrication

Three different devices were fabricated on the glass substrate with SiO_2, 0.01Bi–0.99SiO_2 and $Bi_4(SiO_4)_3$ nanofibers as sensing materials. For this purpose, an array of 100 nm^2 electrodes was formed by a bilayer evaporation of 20 nm of chromium (Cr) followed by 80 nm of nickel (Ni) on a glass substrate. Here chromium acted as a primer and improved the adherence of Ni to the glass substrate. The nanofibers suspensions were prepared in isopropanol solution by ultrasonic agitation and then drop of the prepared suspension was made to fall on the fabricated contacts using a 100 μL micro pipette. The isopropanol evaporated quickly leaving nanofibers in contact between the fabricated contacts on glass substrate. The distance between the contacts was 90 μm for all sensors with almost the equal number of nanofibers is expected in contact between the metal contacts as the nanofibers were deposited in same way with high precision to obtained similar density and distribution of nanofibers on each device. Fig. 1(a) and (b) shows the schematic diagram of final fabricated gas sensing and optical image of the gas sensing device, respectively.

2.3. Measurements

Gas sensors were tested at different gas flow rates. High purity (99.9%) oxygen was used for evaluating sensing behaviour of the fabricated device. Oxygen flow was regulated by 65-mm EW-32044-00 Cole-Parmer Flow metre. It can precisely control the oxygen flow in the range of 0.44–5.05 sccm (standard cubic centimetres per minute or ml/min). Oxygen at different flow rates was

introduced into the testing chamber and AC and DC measurements were performed using Keithley 2400 source metre. All the sensing tests were carried out at temperature range from room temperature (25 °C) to 127 °C using Agilent 4156C parameter analysers with a cryogenic probe station.

3. Results and discussions

Fig. 2(a) shows the FSEM image of SiO_2 nanofibers with polymer. Fig. 2(b)–(d) shows energy dispersive spectroscopy (EDS) and SEM images of xBi–$(1 − x)SiO_2$ nanofibers with $x = 0$, 0.01 and 0.5 heat treated at 600 °C. Before calcination the fibres surface were smooth and bigger in diameter ∼1 μm as shown in Fig. 2(a). But after calcination (600 °C) PVP burn out and the surface becomes rough (inset of Fig. 2(b)–(d)). The typical average length of nanofibers ranges from 100 to 200 μm while the average diameter of nanofibers is 150 nm. EDS spectrum of xBi–$(1 − x)SiO_2$ nanofibers with $x = 0$, 0.01 and 0.5 indicating the presence of silicon, oxygen and bismuth with expected atomic ratios. The EDS spectra show that as bismuth doping increases there is an increase in bismuth content. As bismuth ions replace silicon therefore corresponding decrease in silicon content can also be identified clearly from the EDS spectra. SEM image of $Bi_4(SiO_4)_3$ nanofibers and their corresponding EDS spectra is depicted in Fig. 2(d).

Transmission electron microscope (TEM) images reveal that SiO_2 and $Bi_4(SiO_4)_3$ nanofibers have a porous structure (Fig. 3(a) and (c)). Fig. 3(b) gives the rough estimation of the smooth surface of 0.01Bi–SiO_2 nanofibers at the same resolution. The TEM images indicate that the diameter and length of nanofibers are approximately 150 nm and larger than 150 μm. The obtained results are highly corroborating with the SEM results and verify the uniformity of the nanofibers.

Fig. 4 shows the XRD pattern of pure SiO_2 nanofibers and xBi–$(1 − x)SiO_2$ nanofibers where $x = 0.01$ and 0.5 calcined at 600 °C. For pure SiO_2 one broader peak is observed indicating the amorphous nature of SiO_2 nanofibers. For xBi$(1 − x)SiO_2$ with $x = 0.01$ the SiO_2 crystalline structure is starting to become visible with peak corresponding to (1 0 1) reflections at $2\theta = 25.5°$. It is reported that doping in amorphous SiO_2 may cause physical and chemical disorders. Physical disorder consists of a wide variation in bond angle and bond length, which may cause a change in the electronic structure. The chemical disorder causes a deviation from short range structure in crystalline SiO_2 (as in the case of 0.01 doping). Therefore, it can be concluded that the Bi ions can be incorporated into the SiO_2 lattice [14]. With further increase in bismuth content, evident structural changes are observed in calcined nanofibers. However, when Bi content is 0.5, a well crystalline structure of $Bi_4(SiO_4)_3$ is achieved. For $Bi_4(SiO_4)_3$, nanofibers quite obvious peaks at 21.16°, 24.48°, 27.4°, 32.57°, 34.89°, 43°, 44.9°, 51.79°, 55.03°, 56.60°, 58.12°, 61.10°, 62.56°, 64.0°, 66.76° and 68.16° corresponding to the (2 1 1), (2 2 0), (3 1 0), (3 2 1), (4 0 0), (4 2 0), (4 2 2),